Band nonparabolicities in lattice-mismatch-strained bulk semiconductor layers

R. People and S. K. Sputz
AT&T Bell Laboratories, Murray Hill, New Jersey 07974-2070
(Received 14 August 1989)

Analytic expressions for band nonparabolicities and effective masses are derived for lattice-mismatch-strained bulk semiconductor layers. We have investigated both a full 6×6 valence-band Hamiltonian and an 8×8 model. In the latter, the interactions between the singlet conduction band and the triplet valence bands were treated exactly, with the effects of higher bands calculated to order k^2. To our knowledge, the present work constitutes the first explicit calculation of strain and $\mathbf{k}\cdot\mathbf{p}$ matrix elements using a basis consistent with the formalism of Luttinger and Kohn [Phys. Rev. **97**, 869 (1955)] throughout. The present results should prove to be valuable in determining strained-layer heterostructure band alignments using excitation spectroscopy and in applications requiring highly accurate estimates of confinement energies in narrow quantum-well structures (such as those used in long-wavelength infrared detection).

I. INTRODUCTION

Optical techniques such as photoluminescence excitation spectroscopy[1,2] and optical absorption[3] have been widely used to determine heterojunction band alignments in unstrained semiconductor quantum wells. It is now well known that nonparabolicity plays an important role in determining the subband energies of both very narrow quantum wells (~10 Å) and of higher-lying subbands in wider wells.[4] For isolated quantum wells grown on (001)-oriented substrates, the relevant band nonparabolicity may be obtained via calculation of the energy versus wave vector (k_z) relation to order k_z^4 for the well and barrier bulk materials, i,e.,

$$E_j(k_z)=\frac{\hbar^2k_z^2}{2m^*_{j,z}}(1-\gamma^{(j)}_{\rm NP}k_z^2)\ . \tag{1a}$$

Here E, k_z, and $m^*_{j,z}$ refer to energy, wave vector, and z component of the effective mass. The subscript j is a band index and $\gamma^{(j)}_{\rm NP}$ is the nonparabolicity parameter for the jth band. It should be noted that the use of bulk band nonparabolicities in modeling quantum-well structures is strictly valid only for *isolated* quantum wells. In superlattice structures the subband nonparabolicities tend to be enhanced by zone-folding-induced momentum-space mixing of Γ and X subbands.[5–7] This mixing induces virtual excitations to higher subbands having mixed momentum character, thus altering the matrix elements appearing in $\gamma_{\rm NP}$. Such effects will not be considered in the present work.

Equation (1a) gives two terms in a general power series expansion for the dispersion relation of the jth band. Allowing for $\mathbf{k}=\mathbf{0}$ contributions to $E_j(k)$ and ignoring linear k terms this expansion can be written as

$$E_j(k)\equiv E_0^{(j)}+E_2^{(j)}k^2+E_4^{(j)}k^4+\cdots\ , \tag{1b}$$

where we have dropped the subscript z. The k independent coefficients $E_2^{(j)}$ and $E_4^{(j)}$ are related to the effective mass and band nonparabolicity as follows:

$$E_2^{(j)}\equiv\frac{\hbar^2}{2m_j^*}=\frac{1}{2}\left[\frac{1}{k}\frac{\partial E}{\partial k}\right]\Bigg|_{k=0,E=E^{(j)}(0)}\ , \tag{1c}$$

and

$$E_4^{(j)}\equiv-\frac{\hbar^2}{2m_j^*}\gamma^{(j)}_{\rm NP}=\frac{1}{4!}\left[\frac{1}{k}\frac{\partial^3E}{\partial k^3}\right]\Bigg|_{k=0,E=E^{(j)}(0)}\ , \tag{1d}$$

where $E(k)$ in Eqs. (1c) and (1d) denotes the general secular relation between energy and wave vector as obtained, e.g., using a $\mathbf{k}\cdot\mathbf{p}$ treatment.

Dispersion relations for the degenerate (p-like) valence bands of unstrained bulk group-IV elemental and III-V compound semiconductors may be obtained using the 6×6 $\mathbf{k}\cdot\mathbf{p}$ and spin-orbit Hamiltonian of Luttinger and Kohn,[8] as applied, e.g., by Dresselhaus[9] to Ge. An exact *first-order* treatment of the $\mathbf{k}\cdot\mathbf{p}$ and spin-orbit interactions between the lowest singlet (Γ_2') conduction band of Ge and the triplet (Γ_{25}') valence bands is contained within the later work by Kane.[10] Hasegawa[11] introduced strain into the 6×6 valence-band Hamiltonian at $\mathbf{k}=\mathbf{0}$ in order to interpret the cyclotron resonance experiments of Hensel and Feher[12] on uniaxially stressed Si. Introduction of the spin-orbit interaction splits the sixfold degenerate Γ_{25}' (including spin) valence-band edge at $\mathbf{k}=\mathbf{0}$ into a fourfold $J=\frac{3}{2}$ (Γ_8^v) and a twofold (Γ_7^v) set of states. Unaxial stress

along $\langle 100 \rangle$ or $\langle 111 \rangle$ further splits the fourfold degenerate $J=\frac{3}{2}$ (Γ_8) valence-band edge into two doublets denoted by $(\frac{3}{2},\pm\frac{3}{2})$ and $(\frac{3}{2},\pm\frac{1}{2})$. Each member retains its twofold Kramers degeneracy in the absence of a magnetic field. Hasegawa[11] calculated nonparabolicity corrections to these $J=\frac{3}{2}$ states by treating them to second order in nondegenerate perturbation theory (the states are split by the energy $\Delta E \simeq 2|\epsilon|$ for small stress; where ϵ is the biaxial splitting of the $J=\frac{3}{2}$ set of states). It is presently of interest to obtain a general secular equation for the 6×6 Luttinger Hamiltonian in the presence of lattice mismatch strain without resorting to such approximations. Although it would appear that such a general relation might be readily obtained by combining the $\mathbf{k}=\mathbf{0}$ strain-induced coupling terms calculated by Hasegawa (within the 4×2 cross space between the $J=\frac{3}{2}$ and $J=\frac{1}{2}$ manifolds) along with the explicit $\mathbf{k}$-dependent matrix elements of Luttinger and Kohn;[8] such an approach immediately fails to generate the proper E-vs-$\mathbf{k}$ relationship to order k^2 in the presence of strain. The cause for the breakdown of this approach may be traced to a difference in the form of the *zeroth-order* valence-band basis functions used to block diagonalize the spin-orbit interaction.

In the present work, strain and $\mathbf{k}\cdot\mathbf{p}$ interactions are treated on an equal footing and (following Luttinger) we have chosen the phases of the *zeroth-order* wave functions such that for a given total angular momentum J, the functions corresponding to $+M_J$ and $-M_J$ are related by time-reversal symmetry. This time-reversal degeneracy is of course present because the unperturbed Hamiltonian, which consists of strain, spin-orbit, and $\mathbf{k}\cdot\mathbf{p}$ interactions, is invariant under time reversal.

II. 6×6 VALENCE-BAND DISPERSION WITH STRAIN

For completeness' sake, we reiterate the various contributions to the Hamiltonian for the degenerate valence bands for growth on (001)-oriented substrates:

$$H_v = H_\epsilon + H_{\text{s.o.}} + H_k \tag{2}$$

where the uniaxial strain operator has been given by Kleiner and Roth[13] as

$$H_\epsilon = \tfrac{2}{3}D_u[(J_x^2-\tfrac{1}{3}J^2)e_{xx}+(J_y^2-\tfrac{1}{3}J^2)e_{yy} +(J_z^2-\tfrac{1}{3}J^2)e_{zz}] . \tag{3}$$

In Eq. (3), D_u is the valence-band uniaxial deformation potential for $\langle 001 \rangle$ uniaxial stress and $\mathbf{J}$ denotes the total angular momentum operator divided by $\hbar$. The form of Eq. (3) is particularly simple, since for lattice-mismatched growth on (001) substrates the strain tensor is diagonal having $e_{xx}=e_{yy}=e_{\parallel}$ and $e_{zz}=-(2C_{12}/C_{11})e_{xx}$. The in-plane strain $e_{\parallel}=(a_s-b_0)/b_0$, where a_s is the unstrained lattice parameter of the substrate and b_0 the unstrained lattice parameter of the epitaxial film. Hydrostatic contributions to H_ϵ have been ignored at present. These lead to a rigid shift in the center of gravity of the bands. These terms must be included, however, when conduction-band states (which may have different hydrostatic deformation potentials) are considered, as is shown in Sec. III.

The spin-orbit term ($H_{\text{s.o.}}$) is given by

$$H_{\text{s.o.}} = \frac{\hbar}{4m_0^2c^2}(\sigma\times\nabla V)\cdot\mathbf{p} \tag{4}$$

where σ is the dimensionless Pauli spin matrix vector, V the periodic crystal potential, and $\mathbf{p}$ the particle momentum.

The $\mathbf{k}\cdot\mathbf{p}$ term (H_k) arises naturally given the Bloch form of the carrier wave function.[9] In the present analysis we only require the general form of H_k; since the various constants (inverse mass parameter and momentum matrix elements at zero stress) may be determined either from experiment or calculation. The general form of H_k may be determined using the *theory of invariants,* developed by Luttinger.[14] This approach allows one to write an explicit operator formulation for H_k based upon the angular momentum operator, J_i, in analogy with Eq. (3) for the uniaxial strain Hamiltonian. In the present case

$$H_k = -\frac{\hbar^2}{2m_0}\{\gamma_1K^2-2\gamma_2[(J_x^2-\tfrac{1}{3}J^2)k_x^2+\text{c.p.}] -4\gamma_3(\{J_x,J_y\}\{k_x,k_y\}+\text{c.p.})\} . \tag{5}$$

Here m_0 is the free-electron mass, $K^2=k_x^2+k_y^2+k_z^2$, γ_i are the Luttinger inverse mass parameters (see, e.g., Lawaetz[15]), $\{\,,\,\}$ denotes the anticommutator, and c.p. implies cyclic permutations upon the subscripts x,y,z.

Choosing as basis the six time-reversal symmetry-invariant wave functions

$$\begin{aligned}
\phi_v(\tfrac{3}{2},\tfrac{3}{2}) &= \frac{1}{\sqrt{2}}|(X+iY)\uparrow\rangle ,\\
\phi_v(\tfrac{3}{2},\tfrac{1}{2}) &= \frac{i}{\sqrt{6}}|[(X+iY)\downarrow-2Z\uparrow]\rangle ,\\
\phi_v(\tfrac{3}{2},-\tfrac{1}{2}) &= \frac{1}{\sqrt{6}}|[(X-iY)\uparrow+2Z\downarrow]\rangle ,\\
\phi_v(\tfrac{3}{2},-\tfrac{3}{2}) &= \frac{i}{\sqrt{2}}|(X-iY)\downarrow\rangle ,
\end{aligned} \tag{6a}$$

and

$$\begin{aligned}
\phi_v(\tfrac{1}{2},\tfrac{1}{2}) &= \frac{1}{\sqrt{3}}|[(X+iY)\downarrow+Z\uparrow]\rangle ,\\
\phi_v(\tfrac{1}{2},-\tfrac{1}{2}) &= \frac{i}{\sqrt{3}}|[-(X-iY)\uparrow+Z\downarrow]\rangle ,
\end{aligned} \tag{6b}$$

the 6×6 valence-band Hamiltonian corresponding to Eq. (2) becomes

$$
\begin{array}{cccccc}
(\frac{3}{2},\frac{3}{2}) & (\frac{3}{2},\frac{1}{2}) & (\frac{3}{2},-\frac{1}{2}) & (\frac{3}{2},-\frac{3}{2}) & (\frac{1}{2},\frac{1}{2}) & (\frac{1}{2},-\frac{1}{2}) \\
\left[\begin{array}{cccccc}
H & \alpha & \beta & 0 & \frac{i}{\sqrt{2}}\alpha & -i\sqrt{2}\beta \\
\alpha^* & L & 0 & \beta & i\left[\frac{D}{\sqrt{2}}-\sqrt{2}\epsilon\right] & i\sqrt{3/2}\alpha \\
\beta^* & 0 & L & -\alpha & -i\sqrt{3/2}\alpha^* & i\left[\frac{D}{\sqrt{2}}-\sqrt{2}\epsilon\right] \\
0 & \beta^* & -\alpha^* & H & -i\sqrt{2}\beta^* & \frac{-i}{\sqrt{2}}\alpha^* \\
\frac{-i}{\sqrt{2}}\alpha^* & -i\left[\frac{D}{\sqrt{2}}-\sqrt{2}\epsilon\right] & i\sqrt{3/2}\alpha & i\sqrt{2}\beta & S & 0 \\
i\sqrt{2}\beta^* & -i\sqrt{3/2}\alpha^* & -i\left[\frac{D}{\sqrt{2}}-\sqrt{2}\epsilon\right] & \frac{i}{\sqrt{2}}\alpha & 0 & S
\end{array}\right]
\end{array}
\tag{7}
$$

where

$$
\begin{aligned}
H &= -\frac{\hbar^2}{2m_0}[(k_x^2+k_y^2)(\gamma_1+\gamma_2)+k_z^2(\gamma_1-2\gamma_2)]+\epsilon \equiv H_{\rm hh}+\epsilon \ , \\
L &= -\frac{\hbar^2}{2m_0}[(k_x^2+k_y^2)(\gamma_1-\gamma_2)+k_z^2(\gamma_1+2\gamma_2)]-\epsilon \equiv H_{\rm lh}-\epsilon \ , \\
\epsilon &= \tfrac{2}{3}D_u(e_{zz}-e_{\parallel}) \ , \\
\alpha &= \frac{\sqrt{3}}{m_0}\hbar^2[k_z(k_x-ik_y)\gamma_3] \ , \\
\beta &= \frac{\sqrt{3}}{2}\frac{\hbar^2}{m_0}[(k_x^2-k_y^2)\gamma_2-2ik_xk_y\gamma_3] \ , \\
D &= (H_{\rm lh}-H_{\rm hh}) \ ,
\end{aligned}
\tag{8}
$$

and

$$S=\tfrac{1}{2}(L+H)-\Delta_0 \ .$$

Note that the diagonal components of H_k, namely, $H_{\rm hh}$, $H_{\rm lh}$, and $(H_{\rm hh}+H_{\rm lh})/2-\Delta_0$, gives the dispersion of the heavy-hole $(\frac{3}{2};\pm\frac{3}{2})$, light-hole $(\frac{3}{2};\pm\frac{1}{2})$, and spin-orbit split-off $(\frac{1}{2};\pm\frac{1}{2})$ hole bands to order k^2 in the absence of strain. Note further that the dispersion of the heavy-hole and light-hole bands is anisotropic, having different mass parameters for dispersion in plane [i.e., along $k_{\parallel}=(k_x^2+k_y^2)^{1/2}$] and along the z axis (which is the assumed axis of quantization).

The eigenvalues of Eq. (7) are doubly degenerate. The *general secular equation* is a cubic form given by

$$
\begin{aligned}
0\equiv\Bigg[&-S'H'L'+H'\left[\frac{D}{\sqrt{2}}-\sqrt{2}\epsilon\right]^2 \\
&+|\alpha|^2[\tfrac{3}{2}H'+\tfrac{1}{2}L'+S'-(D-2\epsilon)] \\
&+|\beta|^2(2L'+S'+2D-4\epsilon)+3\sqrt{3}\,\mathrm{Re}[(\alpha)^2\beta^*]\Bigg] \ ,
\end{aligned}
\tag{9}
$$

where $H'\equiv(H-E)$, etc; E denoting the eigenvalue. Since we are only interested in the z dispersion at present we choose $\mathbf{k}=(0,0,k_z)$. Note that in this case $\alpha=\beta=0$ and Eq. (9) reduces to

$$0=H'\left[-S'L'+\left[\frac{D}{\sqrt{2}}-\sqrt{2}\epsilon\right]^2\right] \ . \tag{10}$$

Noting that M_J remains a good quantum number for either (001) or (111) pseudomorphic growths, the three (doubly degenerate) eigenvalues for hole dispersion along k_z are denoted as $E_{3/2}$ and $E_{1/2}(\pm)$. Here

$$E_{3/2}=H\equiv H_{\rm hh}+\epsilon \ , \tag{11}$$

where $H_{\rm hh}(k_z)$ and ϵ have been given in Eq. (8). It is seen that the heavy-hole $(M_J=\pm\frac{3}{2})$ state is strictly parabolic along k_z having an effective mass given by $-(\gamma_1-2\gamma_2)^{-1}$. However, the coherency strain

thoroughly admixes the $(\frac{3}{2},\pm\frac{1}{2})$ and $(\frac{1}{2},\pm\frac{1}{2})$ states, giving rise to two doubly degenerate eigenvalues that may be represented by their M_J values, namely, $\pm\frac{1}{2}$.

The effective mass and nonparabolicities corresponding to the $M_J=\pm\frac{1}{2}$ states may be readily obtained by using the secular E versus k relation implicit in Eq. (10) along with the definitions given in Eqs. (1c) and (1d). One obtains for the strain-dependent hole effective masses:

$$\frac{m_0}{m^*_{\pm 1/2}} \equiv -\frac{2E_{\pm 1/2}(0)(\gamma_1+\gamma_2)+\Delta_0(\gamma_1+2\gamma_2)-\epsilon(8\gamma_2-\gamma_1)}{2E_{\pm 1/2}(0)+\Delta_0+\epsilon} . \tag{12}$$

The nonparabolicities are then given by

$$\gamma_{\rm NP}^{(\pm 1/2)} \equiv \frac{\hbar^2}{2m_0}\frac{\left[\frac{m_0}{m^*_{\pm 1/2}}\right]+2(\gamma_1+\gamma_2)+\left[\frac{m^*_{\pm 1/2}}{m_0}\right](\gamma_1+4\gamma_2)(\gamma_1-2\gamma_2)}{2E_{\pm 1/2}(0)+\Delta_0+\epsilon} , \tag{13}$$

where the $\mathbf{k}=\mathbf{0}$ strain-dependent energies $E^{(0)}_{\pm 1/2} \equiv -\frac{1}{2}(\epsilon+\Delta_0)\pm\frac{1}{2}\Delta_0 F(y)$, with $F(y)=(1-2y+9y^2)^{1/2}$ and $y\equiv\epsilon/\Delta_0$. Equation (12) gives strain-dependent light $(+\frac{1}{2})$ and split-off $(-\frac{1}{2})$ hole masses identical to the results of Hasegawa.[11] The nonparabolicity parameters given in Eq. (13) are general results for the 6×6 valence-band problem and reduce to the results of Hasegawa in the limit of small strains.

The dot-dashed curves in Figs. 1 and 2 show the strain-induced modifications of the z components of the light-hole mass $(m^*_{\pm 1/2})$ obtained using the 6×6 valence-band model given in Eq. (12) for pseudomorphic growth of $In_xGa_{1-x}As$ alloys on (001) GaAs and InP, respectively. The dashed curves in these figures give the unstrained bulk masses as obtained from a linear interpolation between experimental values for the binary compounds.[16] It is observed in Fig. 2 that in-plane compression generates an increase in the z component of the light hole, whereas in-plane tension produces a decrease in this light-hole mass component. The large deviations observed in the pseudomorphic mass values (compared to the unstrained bulk) can lead to substantial errors in calculating quantum confinement energies if strain effects are not properly accounted for. Further, significant deviations from the 6×6 valence-band mass estimates occur when the interactions with the Γ_2' conduction band are included, as is shown in Sec. III.

Strain-induced modifications of the split-off hole mass,

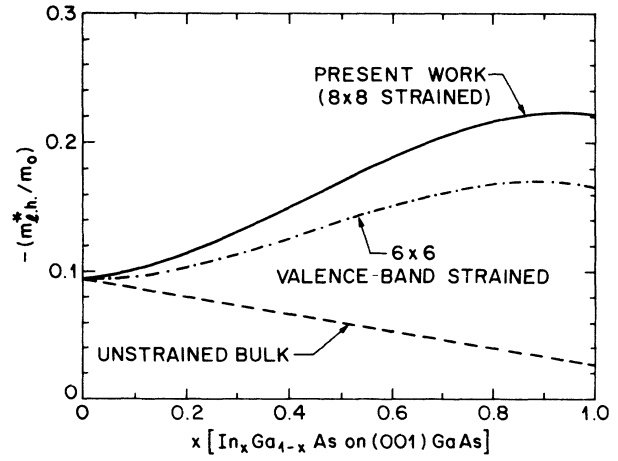

FIG. 1. Light-hole effective masses for $In_xGa_{1-x}As$ layers on (001) GaAs. Dashed curve gives linearly interpolated unstrained mass values; dot-dashed curves give results of the 6×6 (valence band) model with strain, solid curve gives results from 8×8 model.

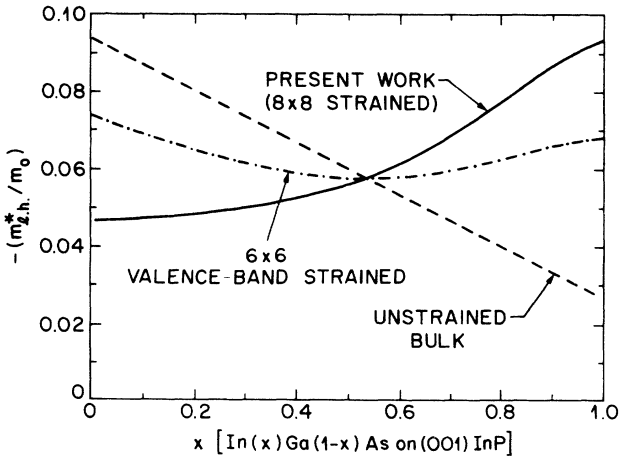

FIG. 2. Light-hole effective masses for $In_xGa_{1-x}As$ layers on (001) InP. Dashed curve gives unstrained mass values used; dot-dashed curves are results for the 6×6 valence-band model; solid curve gives results for the 8×8 model.

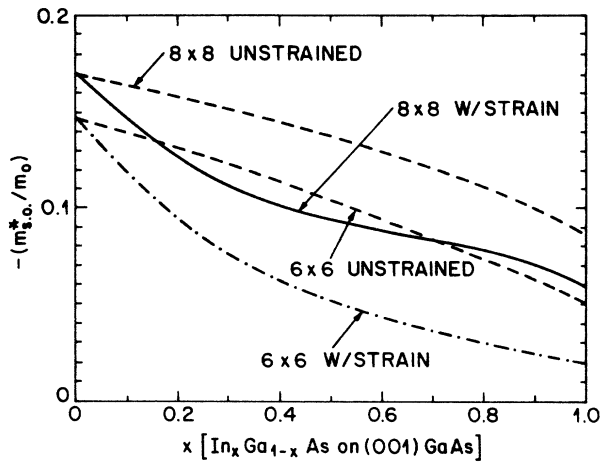

FIG. 3. Split-off hole effective masses for $In_xGa_{1-x}As$ layers on (001) GaAs. Lower dashed curve gives unstrained mass values for 6×6 model wherein $-m_0/m^*_{s.o.}=\gamma_1$. The upper dashed curve gives unstrained mass values for 8×8 model, which involves $\bar{\gamma}_1$ and hence is slightly different even at zero strain. The dot-dashed and solid curves then give strained-layer masses for the 6×6 and 8×8 models, respectively.

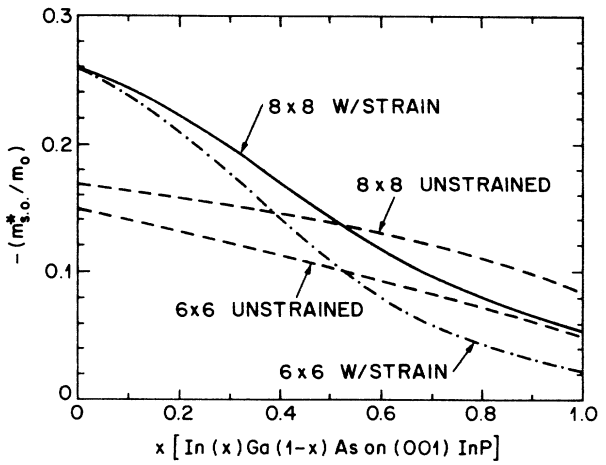

FIG. 4. Split-off hole effective masses for $In_xGa_{1-x}As$ on (001) InP. Curve designations are the same as in Fig. 3.

as predicted by the 6×6 valence-band model, are shown in Figs. 3 and 4 for pseudomorphic growth of $In_xGa_{1-x}As$ allows on (001) GaAs and InP, respectively. The dashed curves labeled "6×6-unstrained" correspond to split-off masses deduced from experimental light-hole $[m^*_{lh}(0)]$ and heavy-hole $[m^*_{hh}(0)]$ masses[2,16] using $m_0/m^*_{s.o.}(0)\equiv\frac{1}{2}[1/m^*_{lh}(0)+1/m^*_{hh}(0)]$. This approach (as opposed to using the theoretical Luttinger parameters) appears to give better agreement with experiment. In Fig. 4 it is seen that in-plane compression decreases the z-component split-off hole mass, while in-plane tension increases this mass component. Hence the behavior of the split-off hole mass in the presence of strain is opposite to that of the light hole (see Fig. 2).

III. SECOND-ORDER KANE MODEL IN THE PRESENCE OF LATTICE-MISMATCH STRAIN

In order to determine strain-dependent conduction-band effective masses and nonparabolicities (near $\mathbf{k}=0$) we introduce two degenerate spin functions having s-like ($L=0$) orbital symmetry, namely $|S\uparrow\rangle$ and $|S\downarrow\rangle$ for the $\phi_c(\frac{1}{2},\frac{1}{2})$ and $\phi_c(\frac{1}{2},-\frac{1}{2})$ conduction-band states, respectively. Again assuming $\mathbf{k}=(0,0,k_z)$ the resulting *second-order* $8\times8\mathbf{k}\cdot\mathbf{p}$ Hamiltonian reduces to two equivalent 4×4 blocks. Lattice-mismatched growth on (001) substrates gives rise to a doubly degenerate (4×4) determinant of the form

$$\begin{array}{c} \begin{matrix} |S\uparrow\rangle & |\frac{1}{2}\frac{1}{2}\rangle & |\frac{3}{2}\frac{1}{2}\rangle & |\frac{3}{2}\frac{3}{2}\rangle \end{matrix} \\ \begin{bmatrix} E_g'+\dfrac{\hbar^2k^2}{2m_0}(1+\tilde{F})-E & \dfrac{1}{\sqrt{3}}kP & -i\sqrt{2/3}kP & 0 \\ \dfrac{1}{\sqrt{3}}kP & \tilde{S}-E & -i\left[\dfrac{\tilde{D}}{\sqrt{2}}-\sqrt{2}\epsilon\right] & 0 \\ i\sqrt{2/3}kP & i\left[\dfrac{\tilde{D}}{\sqrt{2}}-\sqrt{2}\epsilon\right] & \tilde{L}-E & 0 \\ 0 & 0 & 0 & \tilde{H}-E \end{bmatrix} \end{array} \tag{14a}$$

Here $k=k_z$ and $P=\hbar/m_0\langle S|p_z|Z\rangle$. The band gap E_g' is given by

$$E_g'\equiv E_g(0)+(\Xi_d+\tfrac{1}{3}\Xi_u-a_v)\mathrm{Tr}(\vec{e}) \; . \tag{14b}$$

Here $E_g(0)$ is the band gap of the unstrained epitaxial layer with the second term in Eq. (14b) giving the hydrostatic contribution to the band gap of this biaxially strained epilayer. The zero of energy in the strained bulk material has therefore been taken to be coincident with the center of gravity of the valence band.

The determinant in Eq. (14a) differs fundamentally from that of Kane[10] (aside from the inclusion of strain), due to the fact that all matrix elements are calculated to

second order in $\mathbf{k}\cdot\mathbf{p}$ perturbation theory, whereas the Kane model[10] is *first order*. Note that in Ge, e.g., the singlet conduction band [i.e., $\Gamma_2'(\mathrm{CB})$] is within our strongly coupled set of states (which consist of $\{\Gamma_2',\Gamma_{25}^+\}$), and hence the second-order couplings between the $\Gamma_2'(\mathrm{CB})$ and $\Gamma_{25}^+(\mathrm{VB})$ valence-band states must be removed when computing diagonal matrix elements since a given state may only couple to itself via states *outside* the given strongly coupled set of states. When all possible couplings of the $\Gamma_2'(\mathrm{CB})$ and $\Gamma_{25}^+(\mathrm{VB})$ states are considered, the diagonal second-order contributions are usually denoted by the parameter F for the conduction-band state and by the Luttinger inverse mass parameters[15] γ_1, γ_2, γ_3 for the valence-band states. The notation $\tilde{F}$, $\tilde{S}$, etc., in the determinant (14a), signify the removal of all second-order contributions arising from within the present strongly coupled set of states. It may be readily shown[15,17] that the modified $\tilde{F}$ and the modified Luttinger parameters (which we denote by $\tilde{\gamma}_1$, etc.) are related to F and γ_1, γ_2 as follows:

$$\tilde{F}=\frac{2}{m_0}\sum_{j\neq\mathrm{VB}}\frac{|\langle\Gamma_2'(\mathrm{CB})|p_z|\Gamma_{25}^+;j\rangle|^2}{E_j(\Gamma_{25}^+)-E_g^{(0)}}$$
$$=F-\left[\frac{2P^2m_0}{\hbar^2}\right]\Big/E_g^{(0)}\,, \tag{14c}$$

$$\tilde{\gamma}_1=\gamma_1-\frac{2}{3}\frac{P^2m_0}{\hbar^2E_g(0)}\,, \tag{14d}$$

and

$$\tilde{\gamma}_{2,3}=\gamma_{2,3}-\frac{1}{3}\frac{P^2m_0}{\hbar^2E_g(0)}\,. \tag{14e}$$

Also $\tilde{S}=S(\tilde{\gamma}_1,\tilde{\gamma}_2)$, etc. where S, H, L, etc. have been defined in Eq. (8). Note that the sum in $\tilde{F}$ extends over all even parity Γ_{25}^+ states in the conduction band. Since typically such states are very high in energy compared to the band gap of Ge, this term ($\tilde{F}$) will be ignored in the present analysis. Similar considerations apply at the Γ point ($\mathbf{k}=\mathbf{0}$) of the technologically important III-V compounds and hence these compounds may be described by a similar secular determinant. The determinant (14a) therefore leads to the general secular relations

$$E=\tilde{H}=H(\tilde{\gamma}_1,\tilde{\gamma}_2)\,, \tag{15}$$

for the heavy-hole $(\frac{3}{2},\pm\frac{3}{2})$ states [see Eq. (8)] and the cubic form

$$0=\left[E_g'+\frac{\hbar^2k^2}{2m_0}-E\right]\times\left[(\tilde{S}-E)(\tilde{L}-E)-\left[\frac{\tilde{D}}{\sqrt{2}}-\sqrt{2}\epsilon\right]^2\right]$$
$$-\tfrac{1}{3}(kP)^2(\tilde{L}+2\tilde{S}-2\tilde{D}+4\epsilon-3E)\,, \tag{16a}$$

which admixes conduction band (CB), light hole (lh), and split-off (s.o.) hole bands. Again, we note that the heavy-hole $(\frac{3}{2},\pm\frac{3}{2})$ band remains strictly parabolic along k_z. [The heavy-hole band is highly nonparabolic in the (k_x,k_y) plane, however, but such effects are more intimately related to transport rather than optical properties of quantum-well structures.]

The strain-dependent effective mass and band nonparabolicity for the CB, lh and s.o. hole states may be obtained using Eq. (16a) in conjunction with Eqs. (1c) and (1d), respectively. The following general relations are obtained in the presence of lattice-mismatch strain for growth on (001) substrates:

$$\left[\frac{m_0}{m_j^*(\epsilon)}\right]\{3[E_j(0)]^2+2E_j(0)(\Delta_0+\epsilon-E_g')+\Delta_0\epsilon-2\epsilon^2-E_g'(\Delta_0+\epsilon)\}$$
$$=[E_j(0)]^2+E_j(0)(\Delta_0+\epsilon)+\Delta_0\epsilon-2\epsilon^2+[E_g'-E_j(0)][(\tilde{\gamma}_1+2\tilde{\gamma}_2)\Delta_0+2(\tilde{\gamma}_1+\tilde{\gamma}_2)E_j(0)-\epsilon(8\tilde{\gamma}_2-\tilde{\gamma}_1)]$$
$$-\frac{2m_0P^2}{3\hbar^2}[3\epsilon-2\Delta_0-3E_j(0)] \tag{16b}$$

and

$$\gamma_{\mathrm{NP}}^{(j)}\{3[E_j(0)]^2+2E_j(0)(\Delta_0+\epsilon-E_g')+\Delta_0\epsilon-2\epsilon^2-E_g'(\Delta_0+\epsilon)\}$$
$$=-\frac{1}{2}\left[\frac{\hbar^2}{m_0}\right]\left\{\left[\frac{m_j^*(\epsilon)}{m_0}-1\right]\left[\tilde{\gamma}_1[\Delta_0+\epsilon+2E_j(0)]+\tilde{\gamma}_2[2\Delta_0+2E_j(0)-8\epsilon]+\left[\frac{m_0}{m_j^*(\epsilon)}\right][2E_j(0)+\Delta_0+\epsilon]\right]\right.$$
$$+[E_g'-E_j(0)]\left[\left[\frac{m_j^*(\epsilon)}{m_0}\right][\tilde{\gamma}_1(\tilde{\gamma}_1+2\tilde{\gamma}_2)-8\tilde{\gamma}_2^{\,2}]+2(\tilde{\gamma}_1+\tilde{\gamma}_2)+\left[\frac{m_0}{m_j^*(\epsilon)}\right]\right]$$
$$\left.+\left[\frac{2m_0P^2}{\hbar^2}\right]\left[\left[\frac{m_j^*(\epsilon)}{m_0}\right](\tilde{\gamma}_1-2\tilde{\gamma}_2)+1\right]\right\}\,, \tag{16c}$$

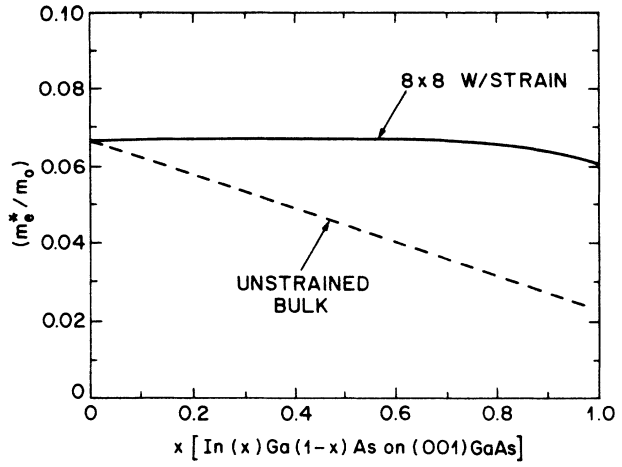

FIG. 5. Electron effective mass for $In_xGa_{1-x}As$ on (001) GaAs. Dashed curve gives unstrained mass values used; solid curve gives results of 8×8 model in the presence of lattice-mismatch strain.

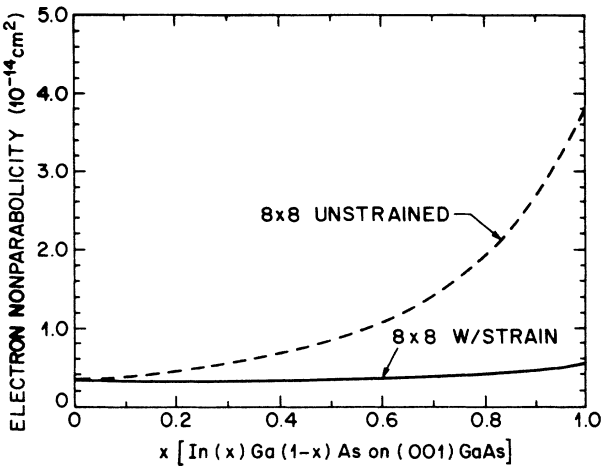

FIG. 7. Electron nonparabolicity (in units of 10^{-14} cm^2) for $In_xGa_{1-x}As$ on (001) GaAs. All results are from 8×8 model.

where j=CB, lh, or s.o., and $E_j(0)$ are the eigenvalues of Eq. (16a) at $k=0$, [namely, E_g' and $E_{\pm 1/2}(0)$ as given in Eqs. (13) and (14b)].

The inclusion of coupling of the degenerate valence bands to the Γ_2' conduction band substantially modifies the light-hole z-mass component, beyond the modifications obtained for the 6×6 VB model. Using Eq. (16b) one can generate the solid curves in Figs. 1 and 2 which show that within the present 8×8 model with strain, the light-hole z-mass component is further enhanced for the case of in-plane compression, whereas in-plane tension further reduces the light-hole z-mass component in comparison to the 6×6 valence-band model. In Fig. 3 we also show the modification of the split-off hole mass z component induced by couplings to the Γ_2' conduction band. The solid curve gives the split-off mass in the presence of strain as obtained from the 8×8 model for pseudomorphic $In_xGa_{1-x}As$ on (001) GaAs. The dashed curve labeled 8×8 unstrained gives the predictions of the 8×8 model in the limit strain tends to zero. Note that in the limit $\epsilon \to 0$ the split-off hole mass is given by $-(\gamma_1)^{-1}$ within the 6×6 model whereas the 8×8 model gives $-[\bar{\gamma}_1 + 2P^2 m_0/3\hbar^2(E_g+\Delta_0)]^{-1}$. These values differ slightly, their difference is therefore reflected in the unstrained mass values for the two models. Similarly, the solid curve in Fig. 4 shows the strain-induced variations in the split-off hole z-mass component for pseudomorphic $In_xGa_{1-x}As$ alloys on (001) InP substrates.

It should be noted that the value for the parameter P^2 used in obtaining the results in Figs. (1)–(4) is deduced from the zero-strain relationship between the conduction-band effective mass $m_e^*(0)$ and P^2. Letting $\epsilon \to 0$ in Eq. (16b) and setting $E_j(0)=E_g$, one obtains $m_0/m_e^*(0) = 1 + 2Pm_0^2(2\Delta_0 + 3E_g)/3\hbar^2 E_g(E_g+\Delta_0)$ where $m_0/m_e^*(0)$ may be obtained from experiment.[16] In

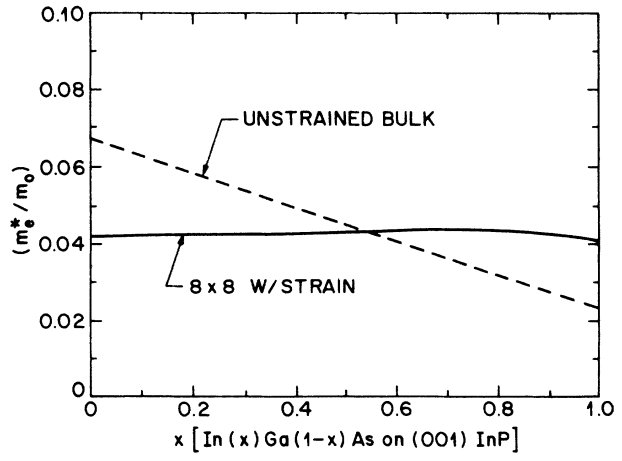

FIG. 6. Electron effective mass for $In_xGa_{1-x}As$ on (001) InP. Curve designations are same as in Fig. 5.

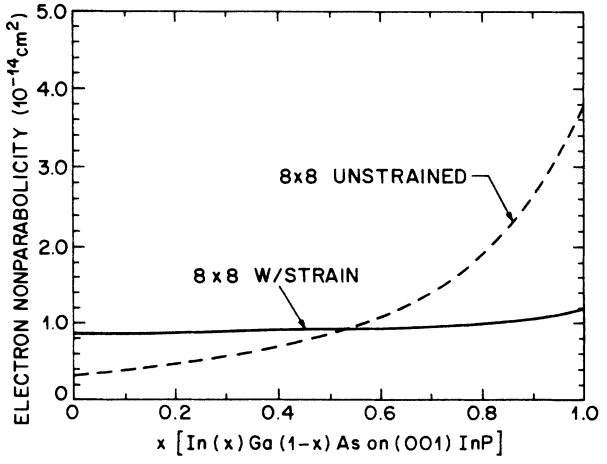

FIG. 8. Electron nonparabolicity (in units of 10^{-14} cm^2) for $In_xGa_{1-x}As$ on (001) InP. All results are from 8×8 model.

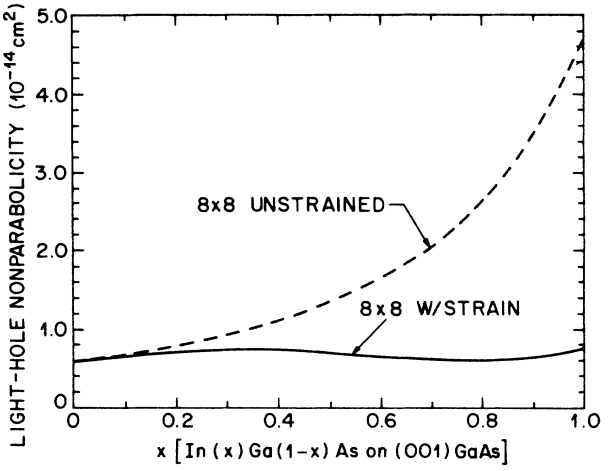

FIG. 9. Light-hole nonparabolicity (in units of 10^{-14} cm^2) for $In_xGa_{1-x}As$ on (001) GaAs. All results are from 8×8 model.

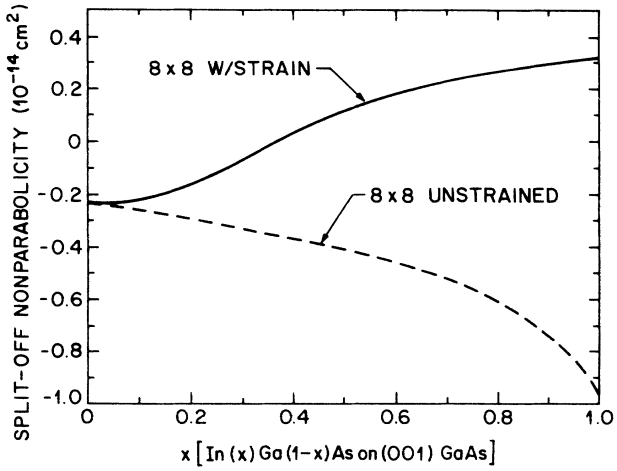

FIG. 11. Split-off hole nonparabolicity (in units of 10^{-14} cm^2) for $In_xGa_{1-x}As$ on (001) GaAs. All results are from 8×8 model.

Figs. 5 and 6 we show linearly interpolated experimental values for the electron effective mass in unstrained bulk $In_xGa_{1-x}As$, plotted as dashed curves. Strain-induced modifications of the electron effective mass are shown in Figs. 5 and 6 (solid curves) for pseudomorphic $In_xGa_{1-x}As$ on (001) GaAs and InP, respectively. The unstrained electron mass change varies between $0.067m_0$ for GaAs and $0.023m_0$ for InAs. However, when $In_xGa_{1-x}As$ alloys are grown pseudomorphically on either GaAs or InP the electron mass becomes essentially independent of composition; its value being given by the unstrained bulk value corresponding to that alloy composition which lattice matches the substrate of interest.

Strained-layer band nonparabolicities for the 8×8 model may be obtained from Eq. (16c). Electron, light-hole, and split-off hole nonparabolicity parameters are obtained by substituting E_g', $E_{+1/2}(0)$, and $E_{-1/2}(0)$ for $E_j(0)$ in (16c), respectively. In Figs. 7 and 8 we show the electron nonparabolicity for pseudomorphic $In_xGa_{1-x}As$ alloys on (001) GaAs and InP, respectively. It is seen that coherency strain essentially removes the compositional dependence of the electron nonparabolicity, $\gamma_{NP}^{(e)}$, which in the presence of strain varies only within 10% of its value at the lattice match composition. In Figs 9 and 10 we show the light-hole nonparabolicity, $\gamma_{NP}^{(lh)}$ for pseudomorphic $In_xGa_{1-x}As$ on (001) GaAs and InP, respectively. Again it is seen that coherency strain greatly reduces the compositional variation of γ_{NP}(lh), in comparison to its value for the cubic (unstrained) alloy. The split-off hole nonparabolicity, γ_{NP}(s.o.), is shown in Figs. 11 and 12, again for pseudomorphic $In_xGa_{1-x}As$ on (001) GaAs and InP respectively. It is observed that both in-plane compression and in-plane tension tend to increase γ_{NP}(s.o.) (relative to its value for cubic material),

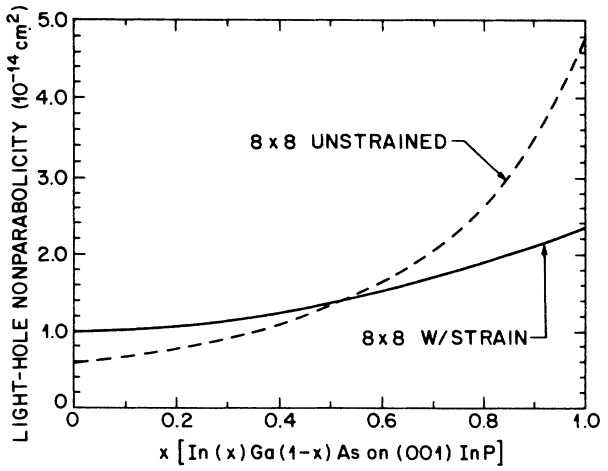

FIG. 10. Light-hole nonparabolicity (in units of 10^{-14} cm^2) for $In_xGa_{1-x}As$ on (001) InP. All results are from 8×8 model.

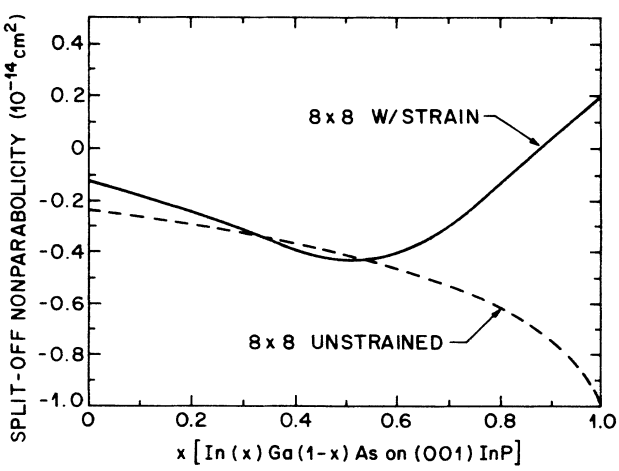

FIG. 12. Split-off hole nonparabolicity (in units of 10^{-14} cm^2) for $In_xGa_{1-x}As$ on (001) InP. All results are from 8×8 model.

whereas in-plane compression, in the main, decreases the electron and light-hole nonparabolicities (as seen in Figs. 8 and 10).

In summary, analytic expressions have been derived for effective masses and band nonparabolicities in lattice-mismatch-strained semiconductor layers. Closed form dispersion relations are obtained using a *second-order* $\mathbf{k}\cdot\mathbf{p}$ model including strain and spin-orbit interactions. Both a 6×6 valence-band model and an 8×8 model (which includes interactions with a singlet conduction-band state) are considered. Considerable differences are found between both light-hole and split-off hole strained-layer masses calculated using the 8×8 model in comparison to the 6×6 (valence band only) model. It is therefore imperative that one uses an 8×8 model when computing confinement masses in strained-layer quantum-well structures such as pseudomorphic $In_xGa_{1-x}As$. It is also found that lattice-mismatch strain tends to remove any compositional dependence of the electron mass in pseudomorphic $In_xGa_{1-x}As$ structures; the electron mass being given essentially by that bulk value corresponding to the lattice-mismatch composition, for a given substrate. This phenomenon (compositional independence) also occurs within the nonparabolicity of the electron and (to a somewhat lesser extent) the light-hole bands.

The present result should prove to be of value in the determination of strained-layer heterostructure band alignments using excitation spectroscopy, and in applications requiring highly accurate estimates of confinement energies in narrow quantum-well structures (such as those used in long-wavelength infrared detection[18]).

ACKNOWLEDGMENTS

We would like to acknowledge helpful discussion with H. Hasegawa and J. C. Hensel. We would also like to thank J. M. Gibson and N. A. Olsson for encouraging the present studies.

[1]R. C. Miller, C. W. Tu, S. K. Sputz, and R. F. Kpf, Appl. Phys. Lett. **49**, 1245 (1986).
[2]D. Gershoni, H. Temkin, M. B. Panish, and R. A. Hamm, Phys. Rev. B **39**, 5531 (1989).
[3]See, e.g., R. Dingle, in Vol. 15 of *Festkörperprobleme,* edited by H. J. Queisser (Pergamon/Vieweg, Braunschweig, 1975), p. 21.
[4]D. F. Nelson, R. C. Miller, and D. A. Kleinman, Phys. Rev. B **35**, 7770 (1987).
[5]L. D. L. Brown, M. Jaros, and D. Ninno, Phys. Rev. B **36**, 2935 (1987).
[6]L. D. L. Brown and M. Jaros, Phys. Rev. B **37**, 4306 (1988).
[7]R. J. Turton, M. Jaros, and I. Morrison, Phys. Rev. B **38**, 8397 (1988).
[8]J. M. Luttinger and W. Kohn, Phys. Rev. **97**, 869 (1955).
[9]G. Dresselhaus, Phys. Rev. **100**, 580 (1955).
[10]E. O. Kane, Phys. Chem. Solids **1**, 249 (1957).
[11]H. Hasegawa, Phys. Rev. **129**, 1029 (1963).
[12]J. C. Hensel and G. Feher, Phys. Rev. **129**, 1041 (1963).
[13]W. H. Kleiner and L. M. Roth, Phys. Rev. Lett. **2**, 334 (1959).
[14]J. M. Luttinger, Phys. Rev. **102**, 1030 (1956).
[15]P. Lawaetz, Phys. Rev. B **4**, 3460 (1971).
[16]See, e.g., *Numerical Data and Functional Relationships in Science and Technology,* Vol. 17a of *Landolt-Börnstein,* edited by O. Madelung (Springer-Verlag, New York, 1982).
[17]C. R. Pidgeon and R. N. Brown, Phys. Rev. **146**, 575 (1966).
[18]See, e.g., B. F. Levine, R. J. Malik, J. Walker, and K. K. Choi, C. G. Bethea, D. A. Kleinman, and J. M. Vandenberg, Appl. Phys. Lett. **50**, 273 (1987).